

DYNAMIC ANALYSIS OF RAILWAY BRIDGES CONSIDERING THE NONLINEAR AMPLITUDE-DEPENDENT SYSTEM BEHAVIOUR - SIMULATION AND IN-SITU TESTS

M. Reiterer¹ and A. Firus²

¹ REVOTEC gmbh
Hermannsgasse 18, A-1070 Vienna
e-mail: michael.reiterer@revotec.at

² iSEA Tec GmbH
Am Flughafen 76, D-88046 Friedrichshafen
andrei.firus@iseatec.de

Abstract

The train-induced forced vibration responses of railway bridges are investigated and evaluated under consideration of nonlinear effects. The considered nonlinearities refer to the amplitude dependency of the natural frequencies, which was observed during in-situ measurements conducted by the authors for several existing railway bridges of different construction type. The nonlinearities detected during dynamic measurements on existing railway bridges are presented and discussed. The focus is on single-span steel and concrete slab bridges with ballasted superstructure. Numerical simulations of train crossings are carried out under assumption of nonlinear beam models for the considered railway bridges. The amplitude dependency of the natural frequencies is considered in these nonlinear simulations and the structural responses during train crossing are presented in the form of resonance curves. For comparison purposes, the calculations are also carried out on linear beam models with constant natural frequencies and the resulting deviations are discussed. The influence of the investigated nonlinearities on the vibration response behavior of railway bridges is highlighted and recommendations for the future consideration of these effects in dynamic calculations of train crossing are given.

Keywords: Railway Bridges, Train Crossing, Train-Induced Vibrations, Nonlinear Effects, Beam Models.

1 INTRODUCTION

According to the currently valid standards [1] and regulations [2], [3], the effects of train-induced vibrations on the serviceability and structural safety of new railway bridges and the dynamic assessment of existing railway bridges must be investigated by means of a dynamic calculation of the train crossings. In [3], [4] and [5] the limit values of 3.5 m/s^2 and 6.0 m/s^2 respectively are defined for the permissible vertical bridge deck acceleration for new bridges and for existing bridges with ballast superstructure. In the dynamic calculation of train crossing, the considered HSLM trains and operating trains are usually assumed as moving individual loads in the sense of a "moving load model" and linear beam or plate models are created for the bridges of interest. The dynamic calculation of the structural responses resulting from train crossing simulations is usually carried out with finite element programs, whereby the equations of motion are solved by application of modal or direct time-step integration. Alternatively, the much more efficient combined numerical and analytical solution methods, such as the analytical time-step integration method presented by Pircher [6] or the DER- and LIR-method presented in ERRI D214/RP 6 [7] are also used.

All train crossing calculation methods applied in the past and currently in practice to determine the vertical structural bridge deck response are based on linear models for the considered railway bridge. The solution methods for linear differential equations of motion are implemented in the common software products and thus time-efficient calculations can be carried out (e. g. application of modal time-step integration). In the recent past, however, significant nonlinear effects have been detected during many dynamic measurements on existing railway bridges, especially regarding the amplitude dependence of the bridge natural frequencies [8]-[12]. In the dynamic measurements on existing railway bridges documented in [8] and [9], forced vibration testing was used to determine the dynamic characteristics and the natural frequencies could be determined by gradually increasing the excitation force amplitude at different levels of the vibration amplitude of the structure. It has been found that an increase of the bridge's vibration amplitudes lead to a decrease of the measured natural frequencies, which may be related to a decrease in the stiffness of the structure during the loading phase. In [10], train acceptance tests were carried out during the commissioning of the new ICE 4 in Germany and a steel bridge susceptible to train induced vibrations was subjected to a detailed analysis of its resonance behaviour during train crossing. These investigations also showed that there was a significant deviation between the theoretically calculated resonance speed and the value determined out of the measurements. The actual resonance speed was significantly lower, and this was attributed, among other things, to occurring nonlinear stiffness effects in the ballast superstructure during train crossing. The theoretical principles of the oscillation behaviour of dynamic systems with an amplitude-dependent natural frequency were presented by Duffing in 1918 [13] and additional theoretical investigations of the Duffing-oscillator were carried out by Parkus [14] and Magnus [15].

In this paper actual findings regarding the nonlinear amplitude dependent behaviour of the natural frequencies of railway bridges during the loading phase are presented and train crossing simulations are carried out considering nonlinear beam models. The results of these simulations are compared to linear bridge model calculations. The amplitude dependence of the natural frequency is considered by a suitable choice of the nonlinear spring characteristic of a boundary restraint modelled at the supporting points of the considered beam. The nonlinear spring law is derived based on measurements already carried out from the authors on existing railway bridges. The effects of nonlinearity and amplitude dependence of the natural frequencies on the forced vibration response of railway bridges during train passage are further investigated.

2 ACTUAL FINDINGS ON NONLINEARITIES IN DYNAMIC MEASUREMENTS

2.1 Nonlinear effects in reinforced concrete slab bridges

In the paper by Vospernig & Reiterer [8], the results of measurement and numerical dynamic investigations carried out on two simple test bridges of identical execution as supported single span reinforced concrete slab bridges are presented. The span of the two identical bridge structures is $l = 8.0$ m, the total length 9.0 m, the structure width 4.50 m, and the slab thickness 0.66 m. With $\rho = 2.5$ t/m³ for the concrete density, this results in a total mass of 66.83 t without any additional masses. The two reinforced concrete slab structures were built side by side on a formwork floor and after curing for 28 days they were supported on prefabricated foundations with four elastomer mats each ($250 \times 300 \times 52$ mm). In the final state of the structure, the mass per unit length including all additional masses like track ballast, sleeper framework and concrete edge beams on both sides, resulted in a total mass per unit length of $\rho A = 12595$ kg/m. The value for the average Young's Modulus of the structural concrete was determined from laboratory tests with $E_{cm} = 29.6 \times 10^9$ N/m². Together with the calculated bending stiffness $E_{cm}I_y = 3191$ MNm² and the span $l = 8.0$ m, the calculated first natural frequency of the vertical bending mode shape under assumption of an uncracked state of the concrete result to $f_{1,ZI} = 12.35$ Hz [8].

The main objective of the investigations carried out in [8] was to determine the dynamic parameters (natural frequencies f_i and the corresponding damping ratios ζ_i) of single span reinforced concrete slab structures at different stages of construction and to investigate the influence of the cracking of the structural slab on the change in the dynamic parameters. For this purpose, dynamic measurements were carried out during the construction of the test bridges, starting from the raw structure up to the final state with the entire superstructure loads. One of the two test bridges was placed in the cracked state after construction by applying a correspondingly high static load. The second test bridge was left in the non-cracked state for the entire duration of the test, so that the results of the two identical executed test bridges could be directly compared and evaluated.

The longitudinal and cross-section of the two test bridges is shown in Figure 1 for the final executed state. The ballast superstructure with sleeper framework was not connected to an existing track and therefore the stiffness contribution of the transition area from the open track to the bridge is not realistically present in the test bridges under investigation.

The forced vibration testing was used to determine experimentally the natural frequencies f_i and the corresponding damping ratios ζ_i for the different assembly conditions of the concrete slab bridges. With two long-stroke vibration exciters in parallel operation, an amplitude-dependent determination of the dynamic characteristics could be carried out by gradually increasing the excitation force amplitude from one measurement to the next in the range of $F_E = 226$ N ÷ 452 N. The gained amplitude-dependent frequency response functions are shown in Figure 2 for the final state of the structure in the non-cracked state (a) and in the cracked state (b). It is seen that the maximum vertical bridge deck accelerations of 0.27 m/s² and 0.37 m/s² were achieved at the highest excitation force amplitude $F_E = 452$ N in the steady state response of the structure. The frequency response functions shown in Figure 2b for the test bridge in the cracked condition (T2) show a significant nonlinearity and amplitude dependence, respectively, in the determined natural frequencies despite the very low vibration amplitudes. When the harmonic resonance excitation with the excitation force amplitude $F_E = 226$ N is applied, the natural frequency of the cracked test bridge is 10.1 Hz. In contrast, applying the higher excitation force $F_E = 452$ N results in a significantly lower first natural frequency of 9.97 Hz. The leftward bending of the frequency response curves is clearly visible here.

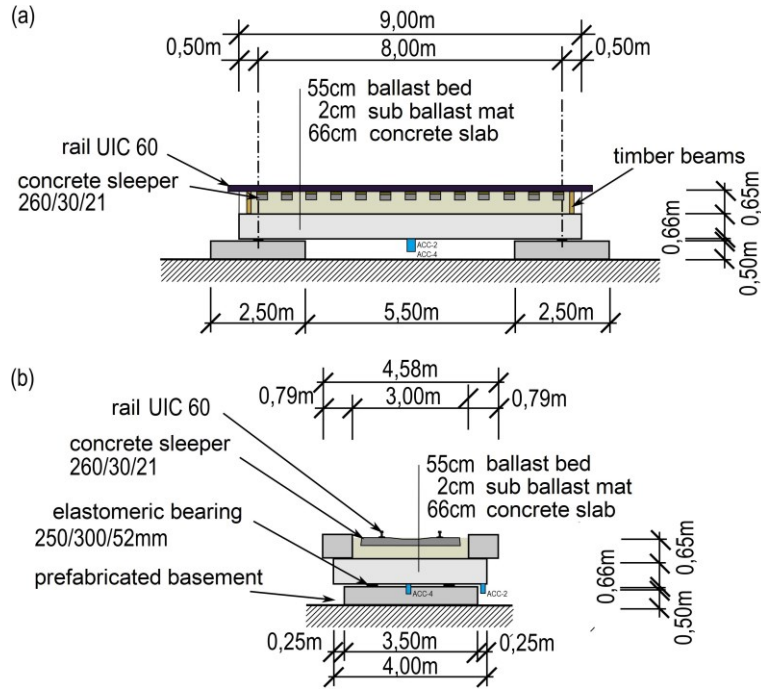


Figure 1: Longitudinal and cross section of the investigated test bridges (only one test bridge is shown; the second test bridge is identical in construction) [8]

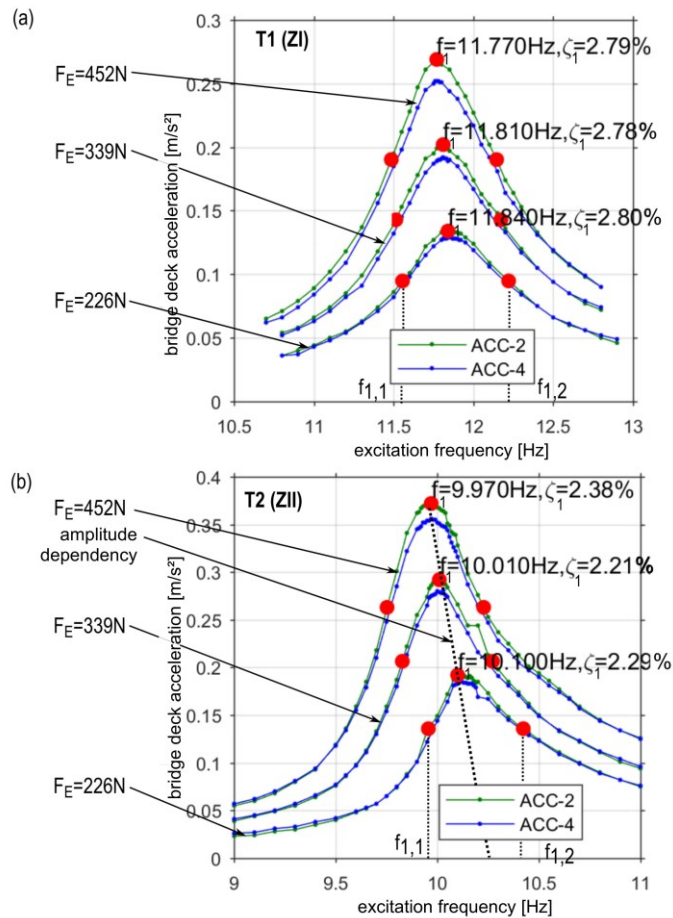


Figure 2: Amplitude dependent frequency response functions in the final state of the two test bridges [8]: a) structure T1 - uncracked state; b) structure T2 - cracked state

In Figure 2a the experimentally gained frequency responses of the test bridge in the non-cracked state also show a non-linearity and amplitude dependence, respectively, of the natural frequency, but this is somewhat lower than in the cracked structure. The test bridge's damping ratios were determined with the half-power bandwidth method, and it does not show any nonlinearities in the amplitude range considered in the measurements. It is assumed that the detected slight differences result from measurement inaccuracies.

It is noted that the amplitude dependence of the natural frequencies of the reinforced concrete slab structures determined from the dynamic measurements can be clearly assigned to a decreasing structural stiffness with increasing vibration amplitude in the case investigated. The kinetic equivalent moving mass of the two test bridges was kept constant in all measurements and the effect of the frequency shift due to the passing train [16], [17], which is often cited in the literature, does not occur here. In the case of the test bridge in cracked condition, the nonlinearity of the natural frequencies is attributed to the crack opening and closing mechanism occurring during the vibration process as well as changes in stiffness at the elastomeric supports. For the non-cracked structure, the nonlinearity is only attributed to stiffness changes in the supports. As the track and superstructure connection to the free track was not executed realistically in the investigated test bridges, no nonlinear effects can be attributed to the transition area here. In the existing structures, however, additional nonlinearities are expected to occur during the passage of the train in the bridge end area due to the changes in the adhesion forces of the ballast grains to each other during the vibration process [18]-[20].

2.2 Nonlinear effects in steel bridges

In [10], the experimental and numerical investigation of a single-span simple supported steel bridge with a span of 19.5 m carried out within the framework of the project "Bridge trafficability" [21] of DB Netz AG is presented. The structure consists of two adjacent identical hollow steel boxes, over each of which a track runs centrally (Figure 3). The two substructures are connected to each other via the ballast superstructure, resulting in coupled vibration modes. The main objectives of the investigation were the verification of the excitation mechanism of the ICE 4, the experimental determination of the resonance curve when excited by the ICE 4 at different crossing speeds, and the analysis of the influence of the longitudinal ballast joint and the ballast bed residual stress on the dynamic behavior of the bridge.

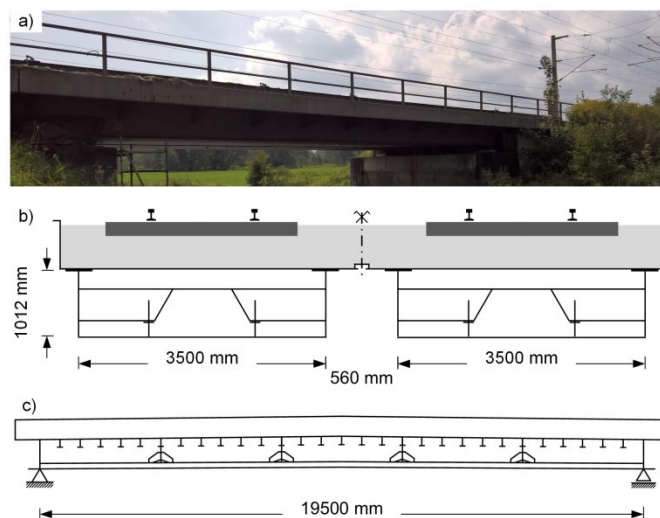


Figure 3: Investigated steel bridge [10]: a) photo caption; b) cross-section at mid-span; c) longitudinal section

Prior to the executed in-situ measurement, an operational modal analysis of the unloaded structure was carried out using the "Reference-Based Combined Deterministic-Stochastic Subspace Identification (CSI/ref)" method implemented in the MACEC software [22]. This resulted in an experimentally determined first natural frequency of the structure of $f_1 = 5.75$ Hz, which can be assigned to the first vertical bending mode. The expected resonance velocity of the considered ICE 4 vehicle can be determined as follows [1]:

$$v_{\text{res}} = f_1 \cdot \frac{L_{\text{üp}}}{i}, \quad (1)$$

where $L_{\text{üp}}$ is the length over the buffer of the coaches and i is an integer between 1 and 4. For $i = 3$ and $L_{\text{üp}} = 28.75$ m, the resulting resonance velocity of ICE 4 is $v_{\text{res}} = 198$ km/h. However, the resonance curve determined from in-situ measurements for excitations by the ICE 4 and shown in Figure 4 shows that the resonance overshoots of the structural response occur at a speed of approx. 171 km/h. This would correspond to a back-calculated natural frequency of the structure of approx. 4.95 Hz, and it differs significantly from the experimentally determined first natural frequency of 5.75 Hz. It can therefore be concluded that the first natural frequency of the structure during train passage is approx. 14 % lower than that of the unloaded structure. Detailed calculations with consideration of the vehicle-bridge interaction [10] have shown that the natural frequency drop caused by the mass effects of the vehicle only plays a minor role. Thus, the significant frequency drop was also attributed to a stiffness reduction, identical to the findings regarding the considered concrete slab bridge in section 2.1. It should be noted at this point that the maximum measured acceleration values, which significantly exceed the limit value of 3.5 m/s^2 [3], had no negative influence on the stability of the bridge's ballast bed. This was observed from visual inspections of the track position after each train crossing.

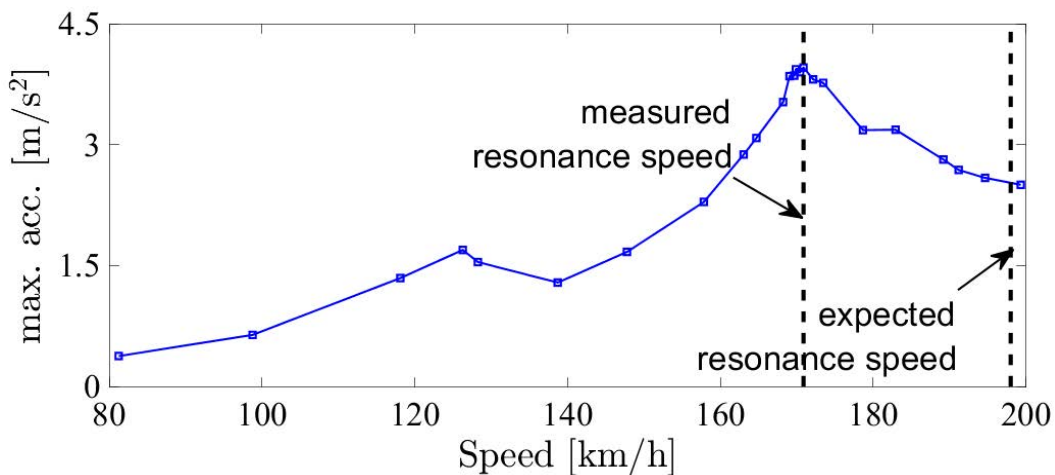


Figure 4: Experimental resonance curve of the considered steel bridge determined for the loaded substructure at midspan of the outer web using train passages of an ICE 4 vehicle [10]

Without going into a detailed discussion here, it should be mentioned that the experimentally determined results for the dynamic characteristic values of railway bridges comprehensively documented in [23] also show a significant reduction in natural frequency with increasing bridge deck vibration amplitudes.

3 LINEAR AND NONLINEAR BRIDGE MODELS FOR TRAIN CROSSING SIMULATIONS

3.1 Linear bridge model for train crossing simulations

In this section the numerical simulations of train crossings are carried out by application of a Finite Element Software and using the direct time step integration method considering a linear beam model for the bridge. All relevant bridge parameters necessary to conduct the numerical simulations are taken from the reinforced concrete slab bridge presented in section 2.1. At first, the numerical calculations are carried out under consideration of the test bridge in the cracked state without taking the non-linear effects into account. The linear numerical model was calibrated to the initial value of the measured first natural frequency $f_0 = 10.10$ Hz (Figure 2b) by properly adjusting the bending stiffness and the stiffness of the additional horizontal spring modelled at the end supports of the beam model. This natural frequency was measured using the forced testing method with the excitation force amplitude $F_E = 226$ N (Figure 2b). The value of the properly adjusted bending stiffness was selected as $(E_{cm}I_y)_{red} = 0.5 \cdot E_{cm}I_y = 1595.5$ MNm² to consider the reduction in stiffness due to cracking [24]. Additionally, to obtain the first natural frequency $f_0 = 10.10$ Hz in the linear numerical bridge model, the stiffness of the horizontal spring at the end supports was chosen to the value 3520 MN/m. Figure 5 shows the numerical model created in the finite element software. The model shown is used to simulate the train crossings in both the linear and nonlinear calculations. For the nonlinear calculations, the spring characteristic is defined as nonlinear (see section 3.2).

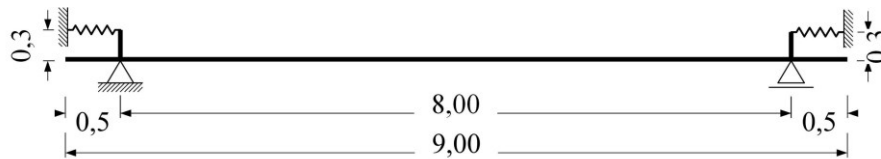


Figure 5: Applied Finite Element model for train crossing simulations of railway bridges (applied for linear and non-linear simulations of train crossing)

The train crossing simulations are carried out with the moving load model according to EN 1991-2 [1], whereby in addition to the standard HSLM-A trains, the operating trains ICE 4 and Railjet, relevant in Germany and Austria, are also considered. For simplification, only the critical model train HSLM-A01 of the ten different HSLM-A trains is considered. This results from the span of the examined reinforced concrete slab structure of $l = 8.0$ m by applying the procedure described in Annex E of EN 1991-2 [1]. The axle loads and axle distances of the operating trains ICE 4 and are taken from RW 08.01.04 [2] and RIL 804 [3].

The train crossing calculations are carried out in the train speed range from 60 to 420 km/h. The speed step is chosen with 5 km/h. The equations of motion are solved by applying the direct time step integration, whereby the time step for the integration is set to $\Delta t = 0.01$ seconds. This captures the contribution of the governing first vibration mode to the bridge's train induced acceleration response with sufficient accuracy. The Rayleigh damping is defined for the first and second natural frequency of the bridge according to EN 1991-2 [1] with $\zeta_{total} = \zeta + \Delta\zeta = 2.56$ %, where $\zeta = 2.34$ % and $\Delta\zeta = 0.22$ %. The evaluation of the maximum vertical bridge deck acceleration is carried out at each velocity step in the middle of the beam structure and the calculation results are used to create a resonance curve for each train type considered. The calculation results are presented and discussed in section 4.

3.2 Nonlinear bridge model for train crossing simulations

The train crossing simulations on nonlinear beam models of the considered reinforced concrete slab bridge are also carried out by applying direct time-step integration with the numerical model shown in Figure 5. Here again, the structure in cracked condition is considered, whereby the nonlinearities (amplitude dependencies) of the natural frequencies are here considered. This is done approximately by two additional nonlinear eccentrically arranged horizontal springs in the support area of the beam model (Figure 5). The definition of a realistic nonlinear spring characteristic for the simulation of train crossings is in itself a very complex task that can only be solved on a structure-specific basis and with a very high experimental effort. In the present case, a simplified approach is followed. Here, the frequency response curves determined from dynamic measurements and shown in Figure 2b are used for the structure in cracked condition. The reductions of the bridge's natural frequencies due to the nonlinear amplitude-dependent behavior can be determined for the measured amplitude range ($a_{1,max} = 0.19 \text{ m/s}^2$ to $a_{3,max} = 0.37 \text{ m/s}^2$) in the form of a negative gradient in the unit $\text{Hz} / (\text{m/s}^2)$ as follows:

$$k_{a3-a1} = \frac{f_{0,3} - f_{0,1}}{a_{3,max} - a_{1,max}} = \frac{9,97 - 10,1}{0,37 - 0,19} \approx -0,70 \frac{\text{Hz}}{\text{m/s}^2}. \quad (2)$$

The derived amplitude dependence of the natural frequency according to Equation 2 is used as a rough orientation value for finding the optimal nonlinear spring characteristic of the considered concrete slab bridge. This step was carried out in an iterative process. It provides for the iterative adjustment of the supporting points of the spring characteristic curve so that the behavior of the numerical model reaches the desired tendency of the frequency reduction. The spring characteristic curve obtained in this way is shown in Figure 6, while the resonance curves obtained with it at different excitation frequencies are shown in Figure 7. It is seen that the (initial) natural frequency drops from approx. 10.1 Hz at 0.5 kN excitation force amplitude to approx. 8.8 Hz at a correspondingly increased force amplitude of approx. 35 kN. A further increase of the force amplitude causes only a relatively small decrease of the natural frequency. Furthermore, it can be observed that the slope of the frequency reduction is on average approx. 0.3 $\text{Hz}/(\text{m/s}^2)$ and is therefore smaller than the experimentally determined negative slope from Equation 2. It should be mentioned that the expected behavior does not show a linear amplitude dependence. In the low amplitude range, as also examined in the measurement results in Figure 2, the frequency reduction can be approximated linearly. For larger amplitudes, the frequency dependence can no longer be represented by the linear relationship.

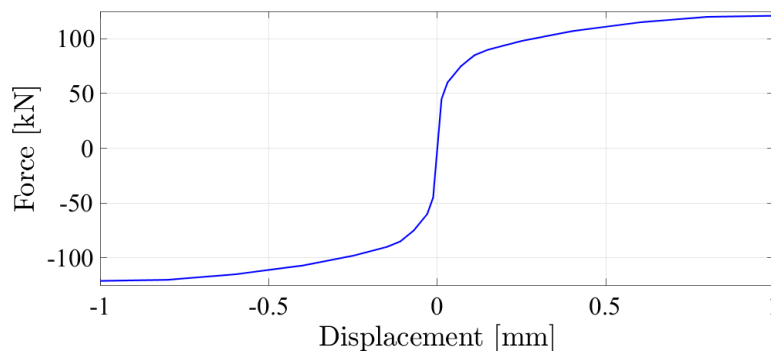


Figure 6: Nonlinear spring characteristic determined from an iterative process

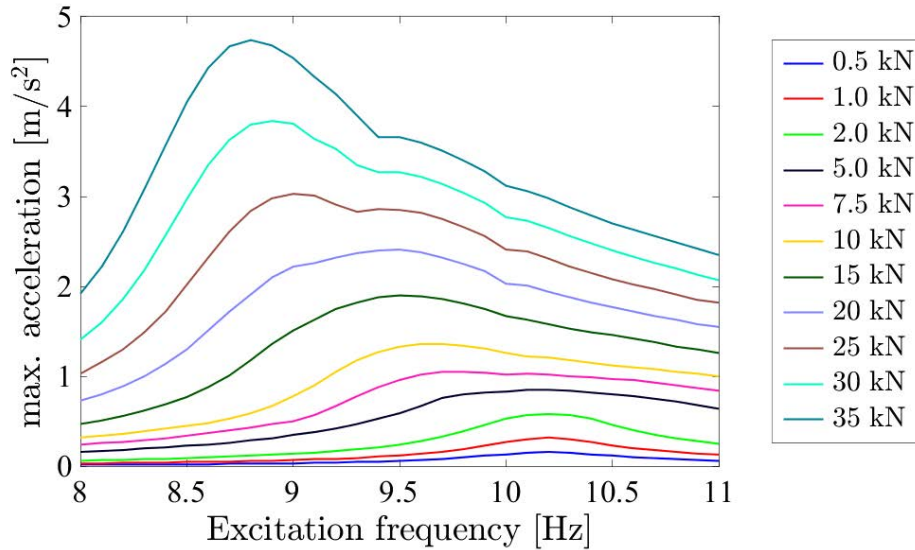


Figure 7: Resonance curves of the nonlinear beam model for harmonic excitation applied at midspan based on the nonlinear spring characteristic curve

4 COMPARISON OF THE RESULTS OF THE NON-LINEAR WITH THE LINEAR BRIDGE MODEL

The dynamic calculations of train crossings on the linear and nonlinear beam model of the investigated reinforced concrete slab bridge results the resonance curves shown in Figure 8 to 10 for the train types considered, HSLM-A01, ICE 4 and Railjet. In the linear beam model, the maximum value of the vertical bridge deck acceleration results 23.8 m/s² for the HSLM-A01 at the corresponding resonance speed of 320 km/h. In comparison, the resonance speed for the simulation of train crossings in the nonlinear beam model is significantly lower at 270 km/h. The reduction of the resonance speed and thus also of the resonance frequency is therefore approx. 16 % due to the considered nonlinear system behavior. At the same time, the maximum value of the vertical bridge deck acceleration of the nonlinear system is with 21.2 m/s² approx. 11 % lower.

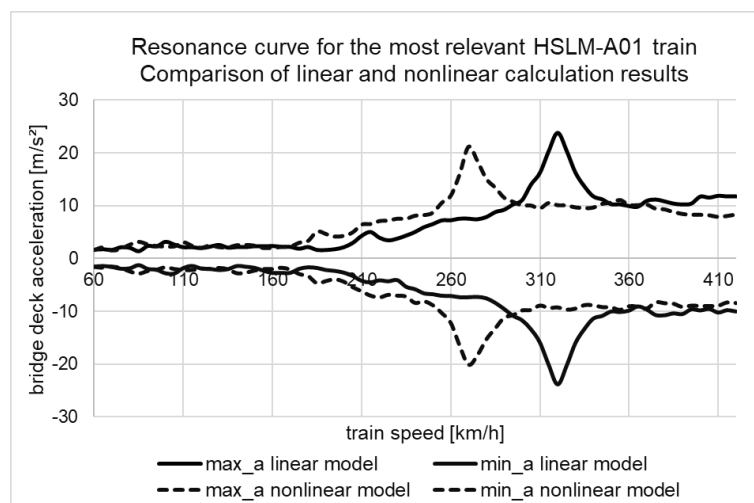


Figure 8: Calculated resonance curves due to crossing of the critical model train HSLM-A01 for the linear and nonlinear bridge model

For the operating train ICE 4, the maximum values of the vertical bridge deck acceleration in the linear and nonlinear beam model are 35.4 m/s^2 and 29.20 m/s^2 respectively. In the nonlinear model, the maximum value is therefore approx. 18 % lower. It is seen from Figure 9 that the simulation of the ICE 4 in the nonlinear model results in a significant reduction of the resonance speed compared to the linear model (from 340 km/h to 285 km/h). The reduction amounts to approx. 16 %.

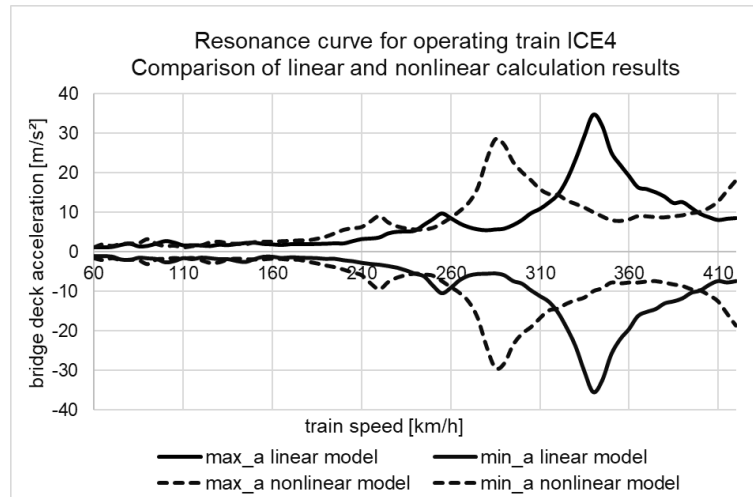


Figure 9: Calculated resonance curves due to crossing of the operating train ICE 4 according to [3] for the linear and nonlinear bridge model

The simulation of the Railjet crossings results in a maximum value of 24.1 m/s^2 for the vertical bridge deck acceleration in the linear beam model at the resonance speed of 315 km/h . In comparison, the nonlinear beam model yields a maximum value of 19.6 m/s^2 at the resonance speed of 265 km/h . The reduction of the resonance speed is therefore approx. 16 % and the reduction of the maximum vertical bridge deck acceleration is approx. 19 %.

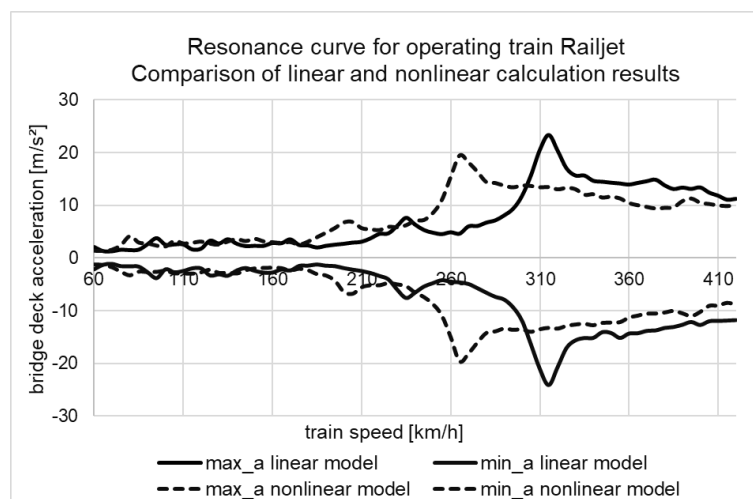


Figure 9: Calculated resonance curves due to crossing of the Railjet (configuration 1 according to [2]) for the linear and nonlinear bridge model

5 CONCLUSIONS

The influence of the observed nonlinear, amplitude-dependent behavior of the resonance frequencies of railway bridges was investigated in relation to the vibration response behavior occurring during train passage. Based on the authors' existing findings on the amplitude dependence of the resonance frequencies, which were determined during executed in-situ measurements on reinforced concrete slab bridges and steel bridges, a non-linear spring law approximating the real behavior was derived and numerical train crossing calculations were carried out. For the numerical calculations, a single-span simple supported reinforced concrete slab was considered, and the crossings were carried out with the HSLM-A01 train, which is critical for the structure, as well as with the operating trains ICE 4 and Railjet in the speed range from 60 km/h to 420 km/h. The linear and non-linear behavior of the train crossings was calculated. The calculation results obtained in the linear and nonlinear beam model for the maximum vertical bridge deck accelerations of the considered railway bridge during train passage show that due to the amplitude dependence of the natural frequencies, a significant reduction of the resonance velocity and lowering of the maximum vibration responses of the bridge results. The reduction of the resonance velocity resulting from the nonlinearity of the resonance frequency is approx. 16 % and this agrees very well with the observations made during in-situ measurements on existing railway bridges. This frequency reduction can play a major role if the calculated resonance velocity is outside the range to be calculated, but the actual resonance velocity falls within the relevant range due to the frequency reduction. The maximum vertical bridge deck acceleration of the structure was determined in the nonlinear beam model with a value up to approx. 19 % lower than in the linear model. The investigations carried out show that considering the nonlinearities of the resonance frequencies determined in in-situ measurements in dynamic calculations of the train passage, a more exact agreement between the measured and the computationally determined vibration response behavior is achieved. The findings presented in the article regarding the significant reduction of the resonance velocity due to the amplitude dependence of the natural frequencies should be taken into account in dynamic calculations of train crossings of railway bridges. However, it should be mentioned that further investigations are necessary in order to develop a generally valid approach for the representation of non-linearities in the dynamic calculation of railway bridges. Nevertheless, the findings of this paper can be used as a rough guide to highlight the extent of the effects of non-linear behavior.

REFERENCES

- [1] ÖNORM EN 1991-2 (2013) *Eurocode 1: Einwirkungen auf Tragwerke – Teil 2: Verkehrslasten auf Brücken (konsolidierte Fassung)*. Austrian Standard Institute, Wien.
- [2] RW 08.01.04 (2011) *Dynamische Berechnung von Eisenbahnbrücken*. ÖBB-Regelwerk. Wien.
- [3] RIL 804: *Richtlinie 804 - Eisenbahnbrücken (und sonstige Ingenieurbauwerke) planen, bauen und instand halten*. DB Netz AG, Jänner 2013.
- [4] ÖNORM EN 1990/A1 (2013) *Eurocode – Grundlagen der Tragwerksplanung – Änderung 1: Anwendung bei Brücken (konsolidierte Fassung)*. Austrian Standard Institute, Wien.
- [5] ÖNORM B 4008-2 (2019) *Bewertung der Tragfähigkeit bestehender Tragwerke - Teil 2: Brückenbau*. Austrian Standard Institute, Wien.

-
- [6] H. Pircher, C. Stadler, J. Glatzl, P. Seitz (2009) *Dynamische Berechnung von Eisenbahnbrücken im Zuge von Hochgeschwindigkeitsstrecken Ein Alternatives Verfahren zur Simulation von Zugüberfahrten*. In: Bautechnik **86**, H. 01, S. 1–13.
- [7] ERRI D 214/RP 6 (1999) *Berechnung einfach gelagerter Brücken bei der Durchfahrt eines Zugverbandes*. ERRI-Sachverständigenausschuss D 214.
- [8] M. Vospernig, M. Reiterer (2020) *Evaluierung der dynamischen Systemeigenschaften von einfeldrigen Stahlbeton-Eisenbahnbrücken*. In: Beton- und Stahlbetonbau **115**, H. 06, S. 424-437.
- [9] M. Reiterer, S. Lachinger, J. Fink, S.-Z. Bruschetini-Ambro (2018) *In-Situ Experimental Modal Testing of Railway Bridges*. In: Proceedings of 18th International Conference on Experimental Mechanics (OCEM 2018), 1-5 July 2018, Brussel, Belgium.
- [10] A. Firus, H. Berthold, J. Schneider, G. Grunert (2018) *Untersuchungen zum dynamischen Verhalten einer Eisenbahnbrücke bei Anregung durch den neuen ICE 4*. In: VDI-Berichte 2321, 6. VDI-Fachtagung Baudynamik, Würzburg, Deutschland, S. 233-248.
- [11] T. Mohamed, K. Abdellatif, B. Mohammed (2021) *Nonlinear analysis of the ballast effect on the dynamics of a simply supported high speed railway bridge*. In: Journal of Applied Sciences **11**, p. 1-20.
- [12] L.R. Ticona Melo, J. Malveiro, D. Ribiero, R. Calcada, T. Bittencourt (2020) *Dynamic analysis of the train-bridge system considering the non-linear behaviour of the track-deck interface*. In: Engineering Structures **220**.
- [13] G. Duffing (1918) *Erzwungene Schwingungen bei veränderlicher Eigenfrequenz und ihre Technische Bedeutung*. Vieweg, Braunschweig.
- [14] H. Parkus (1988) *Mechanik der festen Körper*. Zweite Auflage, Springer Verlag Wien New York.
- [15] K. Magnus (1961) *Schwingungen*. Band 3, B.G. Teubner Verlagsgesellschaft mbH, Stuttgart.
- [16] J. Li, M. Su, L. Fan (2003) *Natural Frequency of Railway Girder Bridges under Vehicle Loads*. In: Journal of Bridge Engineering **8**, H. 4, p. 199-203.
- [17] K. Liu, G. De Roeck, G. Lombaert (2009) *The effect of dynamic train-bridge interaction on the bridge response during a train passage*. In: Journal of Sound and Vibration **325**, p. 240-251.
- [18] T. Rauert, H. Bigelow, B. Hoffmeister, M. Feldmann (2010) *On the prediction of the interaction effect caused by continuous ballast on filler beam railway bridges by experimentally supported numerical studies*. In: Engineering Structures **32**, p. 3981-3988.
- [19] C. Rebelo, S. Da Silva, C. Rigueiro, M. Pircher (2008) *Dynamic behaviour of twin single-span ballasted railway viaducts – Field measurements and modal identification*. In: Engineering Structures **30**, H. 9, p. 2460-2469.
- [20] C. Rigueiro, C. Rebelo, S. Da Silva (2010) *Influence of ballast models in the dynamic response of railway viaducts*. In: Journal of Sound and Vibration **329**, H. 15, p. 3030-3040.
- [21] G. Grunert (2022) *Data and evaluation model for the description of the static–dynamic interface between trains and railway bridges*. In: Engineering Structures **262**, p. 1-19.

- [22] E. Reynders, G. De Roeck (2008) *Reference-based combined deterministic stochastic subspace identification for experimental and operational modal analysis*. In: *Mechanical Systems and Signal Processing* **70-71**, p. 756-768.
- [23] A. Anderson, R. Allahvirdizadeh, A. Kamali, A. Silva, D. Ribeiro, G. Ferreira, P. Montenegro, P. Museros (2021), *High-speed low cost bridges, background report*. Technical Report of the Shift2Rail project (KTH/FEUP/UPV).
- [24] H. Bachmann (2002): *Erdbebensicherung von Bauwerken*. 2., überarbeitete Auflage, Springer Basel AG.